Journal of Applied Chemistry

JAC
http://chemistry.journals.semnan.ac.ir

Synthesis, crystal structure, spectroscopic, molecular docking and DFT Studies of two Schiff base ligands derived from DL-1-Phenylethylamine

Mahdi Salehi[a,*], Maciej Kubicki[b], Mahbobeh Jafari[a], Masumeh Galini[a], Fatemeh Soleimani[a]

[a]*Department of chemistry, Semnan University, Semnan 35351-19111, Iran*
[b]*Faculty of Chemistry, Adam Mickiewicz University, Umultowska 89b, 61-614 Poznan, Poland*

Article history:
Received:06/Nov/2018
Received in revised form: 18/Dec/2018
Accepted: 26/Dec/2018

Abstract

In the present work a new Schiff base ligand was prepared by condensation of 4-hydroxy-3-methoxybenzaldehyde with DL-1-phenylethylamine (HL^1). The product was characterized using FT-IR, ^{1}H-NMR, and UV-Vis spectroscopy. The structure of HL^1 Schiff base ligand was determined by X-ray crystallography. According to this analysis, HL^1 ligand is crystallized in the orthorhombic crystal structure with space group *Pbca*. Also, the structure and electronic properties of HL^2 Schiff base ligand which was synthesized before and HL^1 ligand were analyzed by using DFT calculations. The docking analysis of ligands was reported that bind to the minor and major grooves of B-DNA sequence, respectively.

Keywords: Schiff base, Docking analysis, Crystal structure, DFT study, DL-1 phenylethylamine.

1. Introduction

After the 19th century and the introduction of Schiff bases as ligands, practical applications of them was presented by many researchers [1-4] and interesting field for theoretical studies was developed [5,6]. In recent years, theoretical studies of compounds by means of density functional theory (DFT) calculations have incorporated many considerations in order to interact with their properties and structural features. Moreover, these studies have been widely used for calculating properties of Schiff base compounds and spectroscopic properties of them such as FT-IR, UV-Vis, ^{1}H-NMR, EPR, and Mossbauer spectra, as well as describing the molecular structures and tautomeric equilibrium [7-10].

The results of these studies are in accordance with experimental data. At earlier steps of initiating large-scale theoretical studies, researchers consider thoroughly the optimization of the compounds geometry. Typically, structures predicted by DFT agree closely with results of X-ray diffraction data [11,12]. According to DFT, the calculation of excited states is achieved by time-dependent linear response theory. Time-dependent DFT (TD-DFT) calculations yield the transition energy [13,14].

DFT gains increasing usage in biological systems and chemists trust in the results of DFT calculations to find alternative synthetic routes. Today, theoretical chemistry is used in materials sciences and biochemistry. In this respect, design and synthesis of

* **.Corresponding author:** Associate Professor of Inorganic Chemistry, Faculty of Chemistry, Semnan University, Semnan, Iran.
E-mail: msalehi@semnan.ac.ir

new compounds with unique properties is important in medicinal inorganic chemistry. In addition to Schiff bases role in the development of chemistry, they also are known to have biological activities such as transporting oxygen in biological systems [15], antimicrobial [16-18], antifungal [19], anticancer [20-22], and anti-inflammatory activity [23]. In our recent works, we focused on the synthesis and characterization of new Schiff base ligands [24,25]. In the present study, the synthesis and characterization of two Schiff base ligands ($HL^{1,2}$) derived from 5-bromosalicylaldehyde and 4-hydroxy-3-methoxybenzaldehyde with 1-phenylethylamine are reported (Scheme 1) which HL^1 is a new Schiff base ligand. The structure of new compound is investigated by FT-IR, UV-Visible spectra, and proton nuclear magnetic resonance (^{1}H-NMR). Crystal structure of this Schiff base ligand (HL^1) are characterized by X-ray analysis. In addition, structures of these two ligands are determined and analyzed computationally by B3LYP density functional method and a 6-31G basis set of theory. Also, electronic excitations of complexes are investigated using TD-DFT. Finally, to find out appropriate orientation of them into the binding site of DNA, a powerful computational method, molecular docking, has been used.

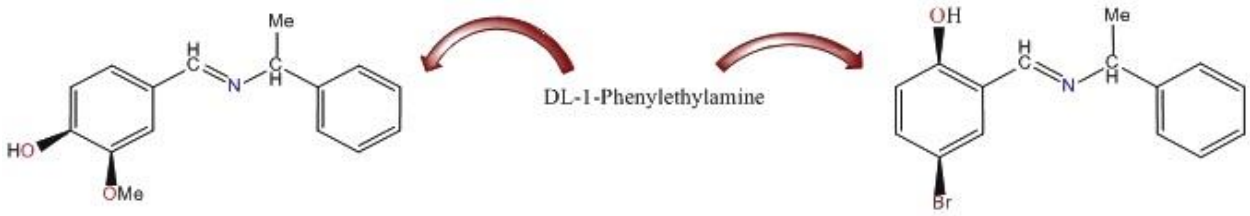

Scheme 1.

2. Experimental

2.1. Materials and Instrumentations

All the chemicals and solvents used in this work were of reagent grade and were used without further purification. FT-IR spectra in KBr plates were obtained on FT-IR SHIMADZU spectrophotometer at 4000-400 cm^{-1}. UV-Vis spectra were recorded on a UV-1650 PC SHIMADZU spectrophotometer in chloroform ($CHCl_3$) solution. ^{1}H-NMR measurements were performed on the NMR BRUKER 300MHz spectrometer using deuterated chloroform ($CDCl_3$) as a solvent.

2.2. Preparation of the Schiff bases ligands

2.2.1. Synthesis of the Schiff-base ligand (HL^1)

The Schiff base ligand, HL^1, was prepared following literature [26]: solution of DL-1-Phenylethylamine (1mmoL) in absolute ethanol (5 mL) was added dropwise to the stirred solution of 4-hydroxy-3-methoxybenzaldehyde (1mmoL) in absolute ethanol (5 mL) and a yellow solution refluxed for 3 h was obtained. The single crystals suitable for X-ray data collection were obtained by slow evaporation of the ethanol solution after 24 h. The crystals were filtered off, washed with a small amount of cold ethanol, and dried under vacuum.

HL^1: Mol. Wt.: 255.31 g/moL. mp. 167˚C. FT-IR: ν_{max} cm^{-1} (KBr): 1629 (s, C=N). UV–Vis: λ_{max} (nm) (ε, $M^{-1}cm^{-1}$) ($CHCl_3$): 349(9000), 301(17900), 268(16200). ^{1}H-NMR ($CDCl_3$, 300MHz): 6.88-7.51(m, 8H), 4.52-4.59(Q, 1H), 1.62-1.64(d, 3H), 3.86(s, 3H), 8.28(s, 1H), 6.70(s, 1H).

2.2.2. Synthesis of the Schiff-base ligand (HL^2)

The Schiff base ligand, HL^2, was prepared following the same procedure as HL^1 except 5-bromosalicylaldehyde was used instead of 4-hydroxy-3-methoxybenzaldehyde [27].

2.3. X-ray crystallography

Diffraction data were collected by the ω-scan technique at 130(1)K (HL^1) on Rigaku SuperNova four-circle diffractometer with Atlas CCD detector and mirror-monochromated CuK_α radiation (λ=1.54178 Å). The data were corrected for Lorentz-polarization as well as for absorption effects [28]. Precise unit-cell parameters were determined by a least-squares fit of 4860 (HL^1)

reflections of the highest intensity chosen from the whole experiment. The structure was solved with SIR92 [29] and refined with the full-matrix least-squares procedure on F^2 by SHELXL-2013 [30]. All non-hydrogen atoms were refined anisotropically, while all hydrogen atoms in HL^1 were found in difference Fourier maps and isotropically refined. Crystallographic data for the structural analysis has been deposited with the Cambridge Crystallographic Data Centre, Nos. CCDC-1548338 (1) and CCDC-1548339 (2). Copies of this information may be obtained free of charge from: The Director, CCDC, 12 Union Road, Cambridge, CB2 1EZ, UK. Fax: +44(1223)336-033, e-mail:deposit@ccdc.cam.ac.uk, or www: www.ccdc.cam.ac.uk . Table 1 present the summery of X-ray structure refinement. All data of HL^2 was reported from reference [27]

Table 1. Crystal data, data collection and structure refinement.

Compound	HL^1	HL^2
Formula	$C_{16}H_{17}NO_2$	$C_{15}H_{14}BrNO$
Formula weight	255.30	304.18
Crystal system	orthorhombic	Monoclinic
Space group	*Pbca*	C2
a(Å)	11.6834	20.890
b(Å)	9.7843	5.7721
c(Å)	23.5483	14.5690
α(°)	90	90
β(º)	90	129.030
γ(°)	90	90
V($Å^3$)	2691.90	1364.7
Z	8	4
D_x(g cm^{-3})	1.26	1.480
F(000)	1088	616
μ(cm^{-1})	0.66	3.97
Θ range (^{0})	3.754, 73.606	3.89, 76.26
Reflections:		
collected	6735	6302
unique (R_{int})	2653 (2.17%)	2609 (1.54%)
with I>2σ(I)	2523	3465
R(F) [I>2σ(I)]	0.0403	0.0384
wR(F^2) [I>2σ(I)]	0.0962	0.0884
R(F) [all data]	0.0364	0.0558
wR(F^2) [all data]	0.0927	0.0965

2.4. Computational methods

All calculations were performed using the Gaussian03 (G03) software package run under Microsoft Windows [31]. Geometry optimization of the structure of ligands ($HL^{1,2}$) was studied using spin-unrestricted DFT to predict the electronic excitations, consisting of solvent effect introduced in the frame of Polarizable Continuum Model (PCM) [32] and using the B3LYP hybrid density functional method. A split-valance double-zeta (6-31G) was used for all atoms. A frequency calculation was done on the optimized structures to represent local minimum on the potential energy surface. In the experimental condition, chloroform was used as a solvent. The natural bond orbital (NBO) analyses [33] were calculated using the NBO 3.1 program as implemented in the Gaussian03 package at the same level of theory and basis set.

2.5. Molecular docking studies of DNA

The crystal structure of dodecamer d(CGCGAATTCGCG)2 (PDB ID: 1BNA) was obtained from the Protein Data Bank (http://www.rcsb.org/pdb). The coordinates of Schiff base ligands $HL^{1,2}$ were taken from its crystal structure as a CIF file and was converted into the PDB format using the Mercury software (http://www.ccdc.cam.ac.uk/).The rigid molecular

docking studies were performed by using AutoDock Tools (ADT) version 1.5.6. The energy calculations were made using genetic algorithms. AutoGrid 4.2 was used to calculate docking area of a grid box of 74 × 64× 117 Å with a grid-point spacing of 0.375 Å.

3. Results and discussions

3.1. Synthesis

The new Schiff base ligands HL^1 was obtained and characterized by FT-IR, ^{1}H-NMR, UV-Vis, and X-ray techniques. The compound appears to be quite stable in the solid state and highly soluble in common solvents like chloroform. Some spectroscopic data for this ligand in Table 2 are in good agreement with the expected values.

Table 2. Spectroscopic data for ligands.

Compound	Selected IR[a] $\upsilon_{(C=N)}$	^{1}H-NMR (δ, ppm)[b]	UV-Vis: λ_{max} (nm) (ε, M^{-1} cm^{-1})[c]
HL^1	1629	6.88-7.51(m, 8H), 4.52-4.59(Q, 1H), 1.62-1.64(d, 3H), 3.86(s, 3H), 8.28(s, 1H), 6.70(s, 1H)	349(9000), 301(17900), 268(16200)
HL^2	1631	4.55-7.40 (m, 8H), 8.33 (s, 1H), 13.58(s, 1H), 1.63-1.66 (d, 3H), 4.55-4.61 (q, 1H)	280(74600), 331(3300), 381(18200)

[a] KBr pellets, [b] Solvent is $CDCl_3$, [c] Solvent is chloroform.

3.2. Spectroscopic characterization of the ligands

3.2.1. FT-IR spectra and Electronic spectra

The FT-IR spectra of the two Schiff base ligands show strong sharp absorption bands at 1631 (HL^2) and 1629 (HL^1) cm^{-1} indexed to the (C=N) band. Other stretching vibrations at 1276 and 1278 cm^{-1} were indexed to the phenolic (C-O) stretch of $HL^{1,2}$, respectively [34-35]. The electronic absorption spectra of the Schiff base free ligands in $CHCl_3$ solution are shown in supplementary and the spectral data are presented in Table 2. The electronic spectrum consists of two bands centered at 280 and 331 nm related to the HL^2 ligand and two bands centered at 268 and 301 nm related to the HL^1 ligand, attributed to the intra ligand $\pi\rightarrow\pi^*$ transitions. A third band in the electronic spectrum of the $HL^{1,2}$ ligands at 381 and 349 nm is assigned to the $\pi\rightarrow\pi^*$ transition, respectively.

3.2.2. ^{1}H-NMR spectra of ligands

The ^{1}H-NMR spectral measurements of ligands $HL^{1,2}$ were performed in $CDCl_3$ solution. In the ^{1}H-NMR spectrum of HL^2, the signal appearing as a singlet at 8.33 ppm is assigned to the azomethine group proton (Fig. 1). The signals due to the aromatic protons of two phenyl rings are observed in the 6.86-7.40 ppm range. Also, the phenolic OH signal was evidenced at 13.58 ppm, methyl protons appeared within 1.63-1.66 ppm, and a quartet peak was observed within the 4.55-4.61 ppm region corresponding to the HC-Me. The ^{1}H-NMR spectral data of HL^1 show features similar to those observed for HL^2: The signal at 8.28 ppm is assigned to the azomethine group proton and those observed in 6.88-7.51 ppm are due to the aromatic protons. The single the methyl protons appeared at 1.62-1.64 ppm. On the other hand, a quartet peak observed in the 4.52-4.59 ppm region corresponds to HC-Me. The additional signals at 3.86 and 1.62 ppm are indexed to the -O-CH_3 and C-Me protons, respectively (Fig. 2).

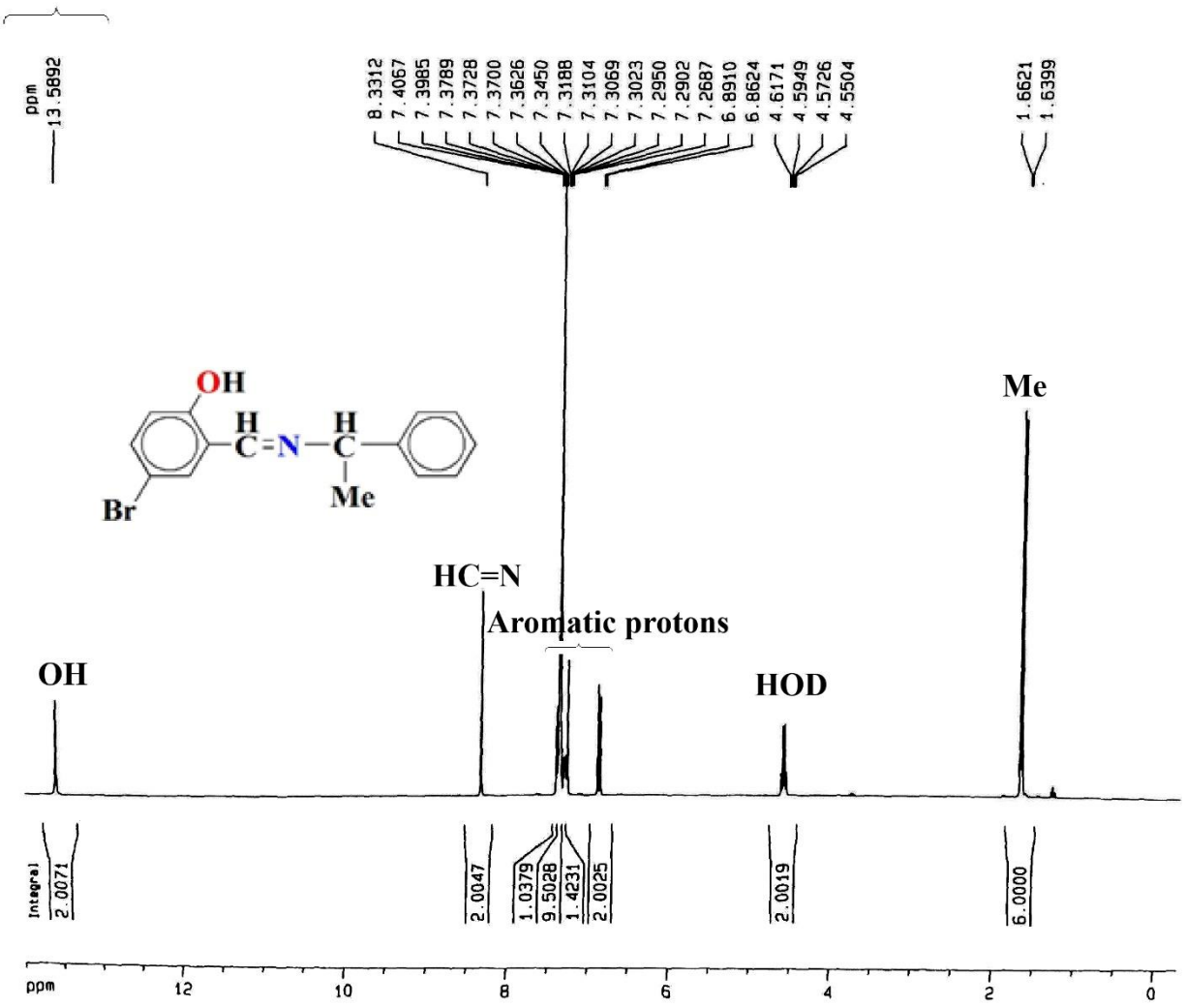

Fig. 1. ^{1}H-NMR spectrum of HL^{2} in $CDCl_3$.

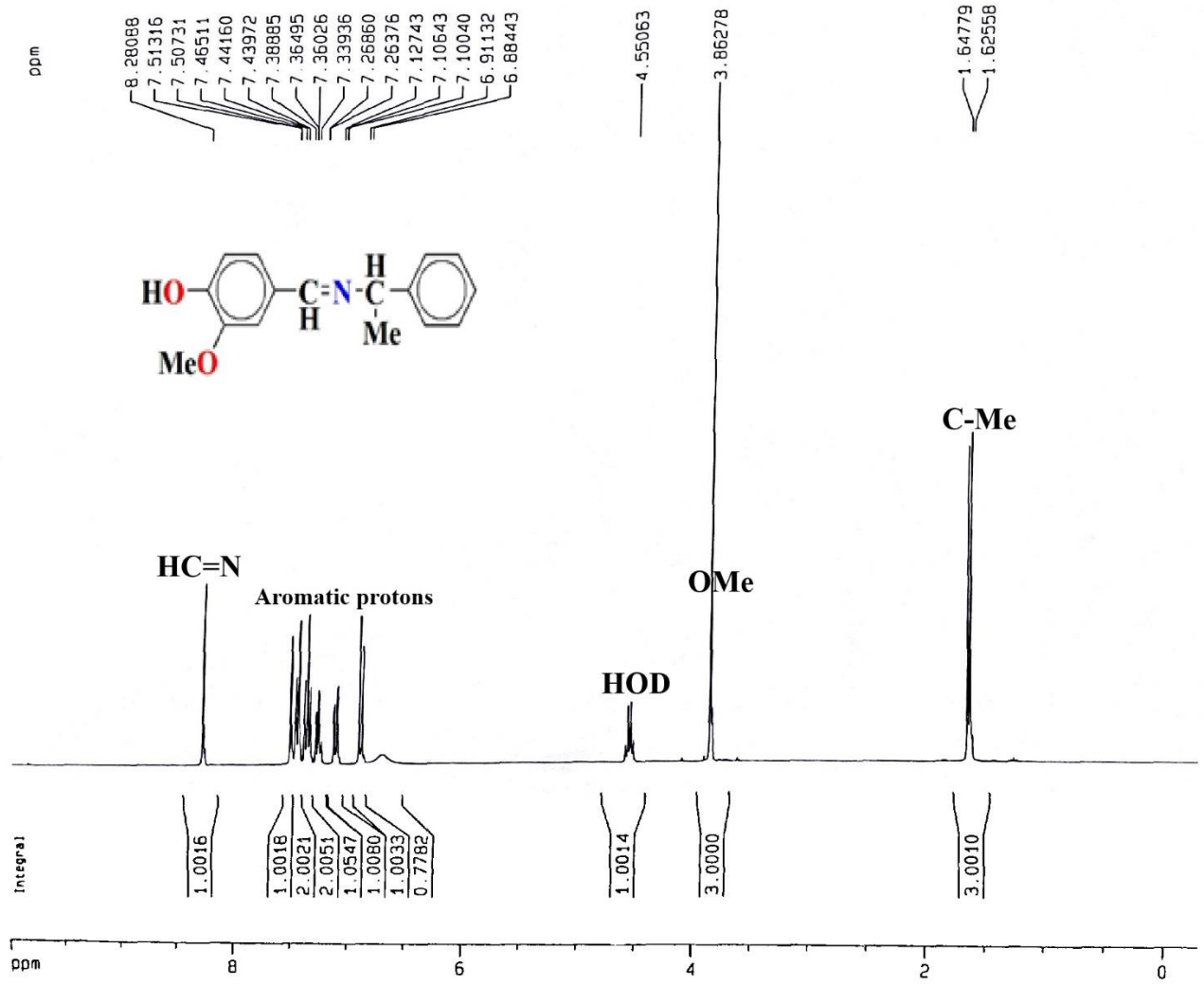

Fig. 2. ^{1}H-NMR spectrum of HL^1 in $CDCl_3$.

3.3. Description of the crystal structure

The perspective view of the molecule HL^1 is shown in Figure 3, respectively. Table 3-6 presents relevant bond lengths and angles of HL^1 and HL^2. HL^1 molecule is chiral at C7 and due to the centrosymmetric space group, both enantiomers are present, exactly in 1:1 ratio. The values of the overall conformation of the molecule in HL^1 is 58.95(4) º. In HL^1 there are relatively strong O-H···N intermolecular hydrogen bonds, which connect molecules into infinite chains; a number of C-H···O and other interactions are involved in the three-dimensional structure. Hydrogen bond data are listed in Table 7.

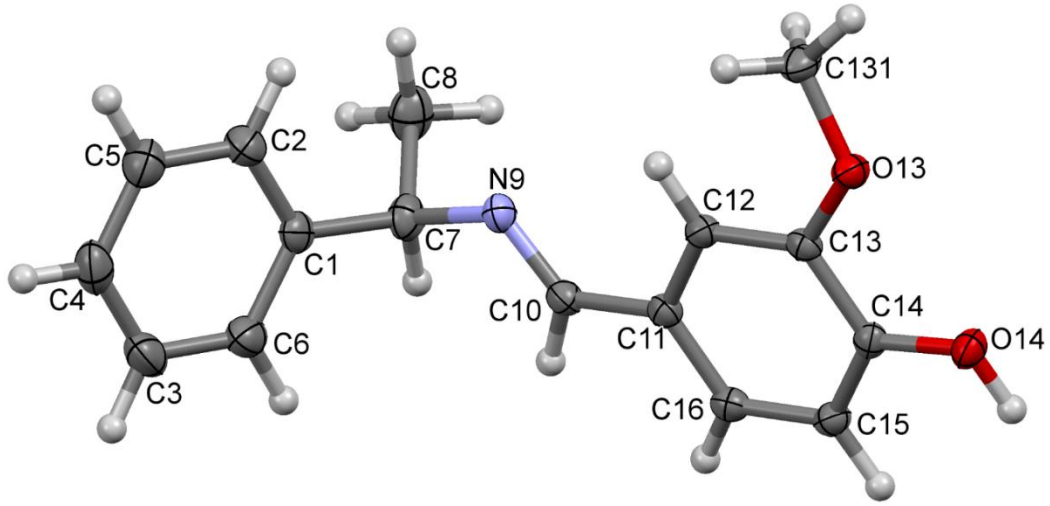

Fig. 3. A perspective view of HL^1; ellipsoids are drawn at the 50% probability level; hydrogen atoms are shown as spheres of arbitrary radii.

Table 3. Selected experimental and calculated bond lengths of HL^2 (Å).

atom	6-31G	6-311++G**	X-ray
C_1-C_2	1.4024	1.3992	1.3867
C_{12}-N_{18}	1.4643	1.4642	1.4741
C_{18}=N_{19}	1.2837	1.2794	1.2699
C_{21}-C_{22}	1.4202	1.4174	1.4077
C_{22}-O_{23}	1.3454	1.3408	1.3420
C_{29}-Br_{30}	1.9082	1.9189	1.8986
O_{23}-H_{24}	0.9985	0.9945	0.7936
C_{31}-H_{32}	1.0864	1.0837	0.9299

Table 4. Selected experimental and calculated angles of HL^2 (°).

atom	6-31G	6-311++G**	X-ray
C_6-C_8-C_{10}	120.0228	120.02784	119.8506
C_{12}-C_{14}-N_{18}	108.9743	109.07611	108.69148
C_6-C_4-H_5	120.0550	120.0219	119.8537
C_{21}-C_{22}-O_{23}	122.0650	121.8508	121.9033
Br_{30}-O_{29}-C_{27}	119.6344	119.6002	119.3573

Table 5. Selected experimental and calculated angles HL^1 (°).

atom	6-31G	6-311++G**	X-ray
C_6-C_8-C_{10}	120.3312	120.7034	120.7034
C_{12}-C_{19}-N_{18}	118.1577	116.0468	116.04680
C_{30}-O_{31}-H_{32}	108.439	112.1068	112.10684
C_5-C_4-C_6	120.1643	120.4376	120.43763
C_{24}-O_{25}-C_{26}	117.6807	117.0883	117.08826

Table 6. Selected experimental and calculated bond lengths of HL^1 (Å).

atom	6-31G	6-311++G**	X-ray
C_1-C_2	1.3996	1.3938	1.3938
C_{12}-N_{18}	1.4585	1.4834	1.4834
C_{18}=N_{19}	1.2754	1.2768	1.2768
C_{12}-C_{14}	1.5415	1.5220	1.5220
C_{30}-O_{31}	1.3627	1.3509	1.3509
C_{26}-O_{25}	1.4187	1.4281	1.4281
O_{31}-H_{32}	0.9701	0.9375	0.9375
C_4-H_5	1.0871	0.9753	0.9753

Table 7. Hydrogen bond data (Å, º)

D	H	A	D-H	H···A	D···A	D-H···A
			HL2			
O12	H12	N9	0.80(5)	1.85(5)	2.599(4)	156(5)
			HL1			
O14	H14	N9^{i}	0.939(19)	1.782(19)	2.7124(13)	170.5(16)

3.4. Theoretical studies

DFT studies showed monoclinic and orthorhombic crystallography systems for optimized structures of $HL^{1,2}$ that were accordance with results of X-ray crystallographic analysis (Fig.s 4 and 5). Table 3-6 presents some selected optimized and experimental bond lengths and angles for $HL^{1,2}$ compared to experimental results. As can be seen, there is a good agreement between theoretical and experimental values. The differences, on the other hand, can be attributed to the environmental effects as well as the choice of DFT method [36,37]. To reach more precious amounts for bond lengths and angles, a more exact method was employed; i.e., B3LYP/6-311++G**. Using this method, a stronger agreement was seen between the numerical and experimental values. Also, the structures of $HL^{1,\ 2}$ were determined computationally at the B3LYP/6-31G level of theory. Frequency calculations confirmed that the optimized structures of $HL^{1,\ 2}$ resided in a local minimum of the potential energy surface. The sum of Mulliken atomic charge calculated NBO of $HL^{1,2}$ is zero. The comparison between experimental and DFT calculation of bond length shows that the length obtained from 6-311++G** is in good agreement with experimental data. The other part of calculations (HOMO and LOMO) refers to molecular orbitals. These so-called frontier orbitals parameters are important in quantum chemistry. The energy gap between HOMO and LUMO characterizes the molecular chemical stability. When this distance is low, the molecule has a high activity, chemical hardness, and EH-L, suggesting the lower reactivity of molecule [38, 39]. The HOMO energy level for HL^2 is -0.22139 a.u (-6.02424 eV) while the LUMO energy level is -0.06268 (-1.705585 eV). The orbital energy level analysis for the ligand at the B3LYP level shows that the HOMO–LUMO gap is 4.318 eV. The HOMO energy level for HL^1 is -0.20538 a.u (-5.5886 eV) while the LUMO energy level is -0.03376 (-0.91864 eV). Moreover, the orbital energy level analysis for the ligand at the B3LYP level shows that the HOMO–LUMO gap is 4.66 eV. To interpret experimental UV-Vis spectra of the $HL^{1,\ 2}$, TD-DFT calculations were used. Figures 5 and 6 present comparison of the calculated and experimental UV-Vis spectra of the ligands. The calculated electronic spectroscopy data and isodensity plots of HOMO, HOMO-1, HOMO-2, LUMO, LUMO+1, and LUMO+2 for both ligands are presented in Table 8, 9, 10, and 11, respectively. For both ligands, as it could be seen in Table 8 and 9, the major contributions in the HOMO and LUMO were from π and π^*. Also, Table 10 and 11 show close accordance between experimental and DFT calculated data, respectively.

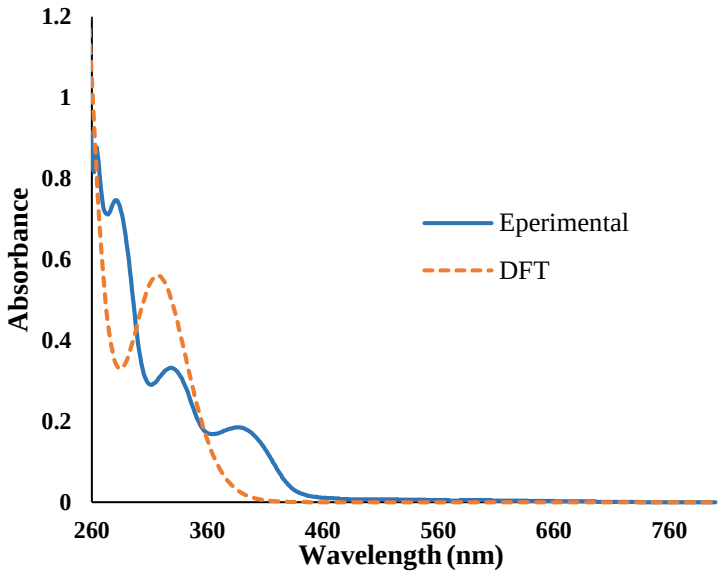

Fig. 4. Experimental and calculated electronic spectra of HL^1**.**

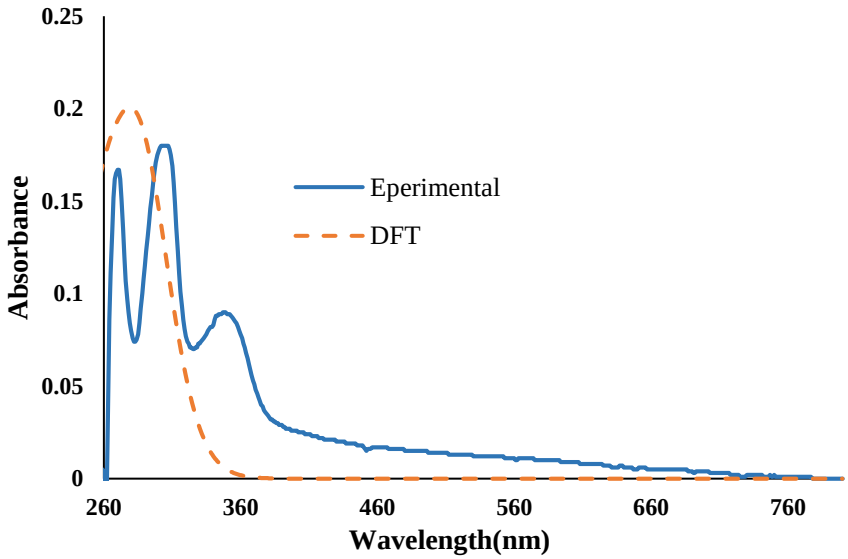

Fig. 5. Experimental and calculated electronic spectra of HL^2

Table 8. Surface plots of the molecular orbitals and optimized geometry of HL^1 along with the orbital composition.

Molecular Orbitals		Energy(eV)
HOMO	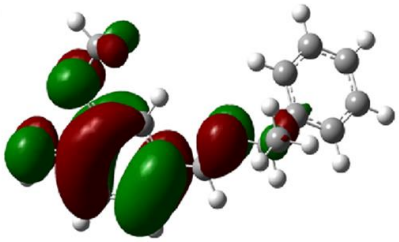	-5.5886 eV
HOMO-1	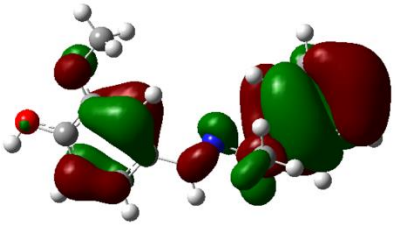	-6.3611 eV
HOMO-2	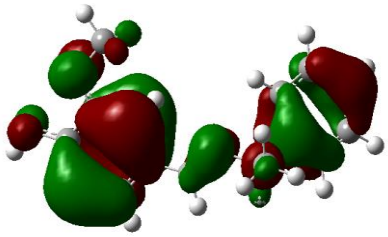	-6.4220 eV
LUMO	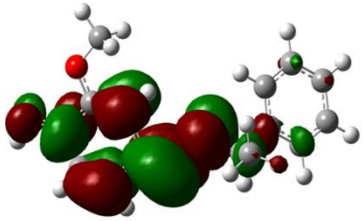	-0.91864 eV
LUMO+1	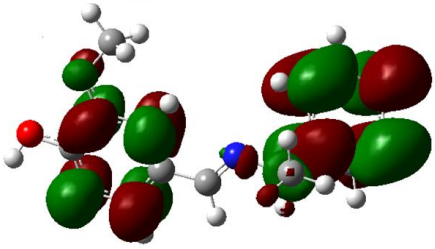	0.2046 eV
LOMO+2	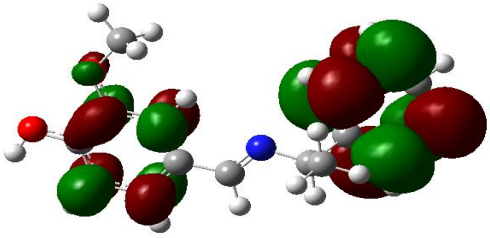	0.2193 eV

H=HOMO, L= LUMO, H-1 = HOMO-1, L+1 = LUMO+1, F: Oscillator strength

3.5. Molecular docking

Molecular docking technique can be used to predict the affinity and activity and the binding orientation of small molecule drug. Hence docking plays an important role in the rational design of drugs. To provide theoretical insight into the interaction between Schiff base ligands and DNA, ligands were docked within the DNA duplex of sequence d(CGCGAATTCGCG)2 dodecamer (PDB ID: 1BNA). From the data presented in Table 12, the Schiff base ligands the HL^1 and the HL^2 showed interaction with minimum binding energy of -6.99 and -7.27 kcal mol^{-1} with the crystal structure of DNA, respectively. The more negative relative binding energy for Schiff base HL^2 indicated greater binding tendency of this compound with DNA. Fig. 6 shows the Schiff base ligands HL^1 and the HL^2 fit into the minor and major grooves of the DNA, respectively [40]. Also, the resulting docking in which the ligands HL^1 and the HL^2 binds into the DNA by hydrogen bonds (Fig. 7). The hydrogen bond for HL^1 is between the O of OH with DA118 (2.35Å). Whereas, the four hydrogen bonds are assigned for HL^2. The three hydrogen band display between O of OH with DG110 and phosphate (2.01 Å, 1.92 and 2.46 Å). In addition, there is one hydrogen band between the nitrogen atom of imine and phosphate (3.01Å).

HL **1**	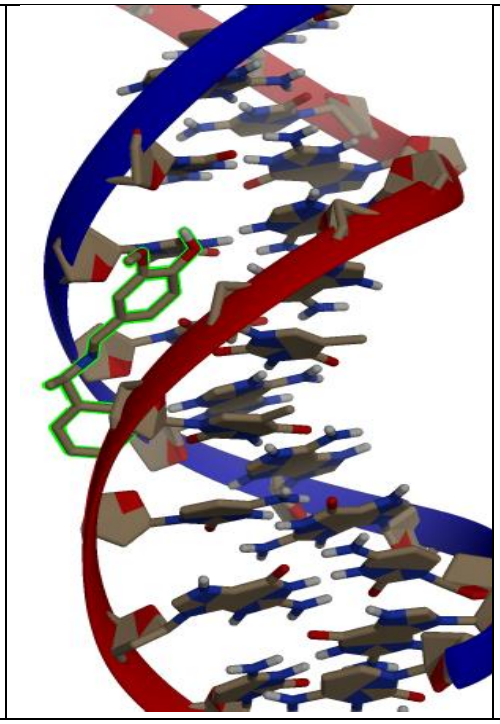	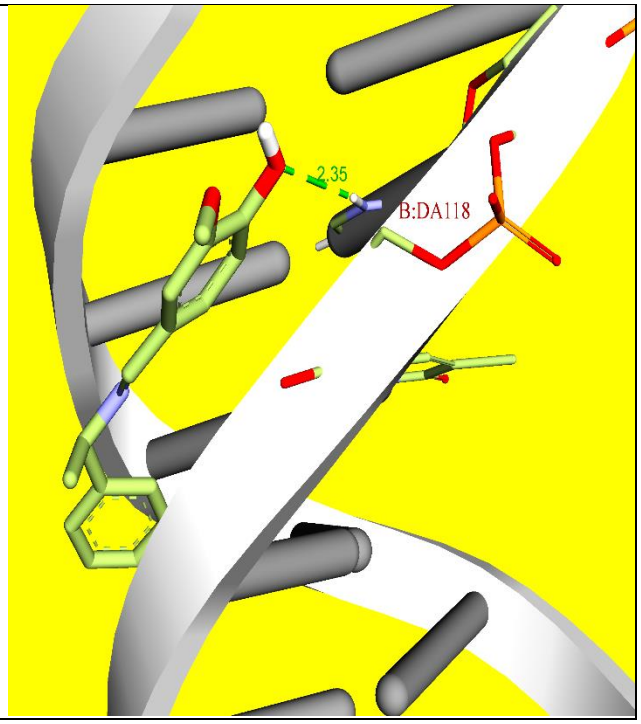

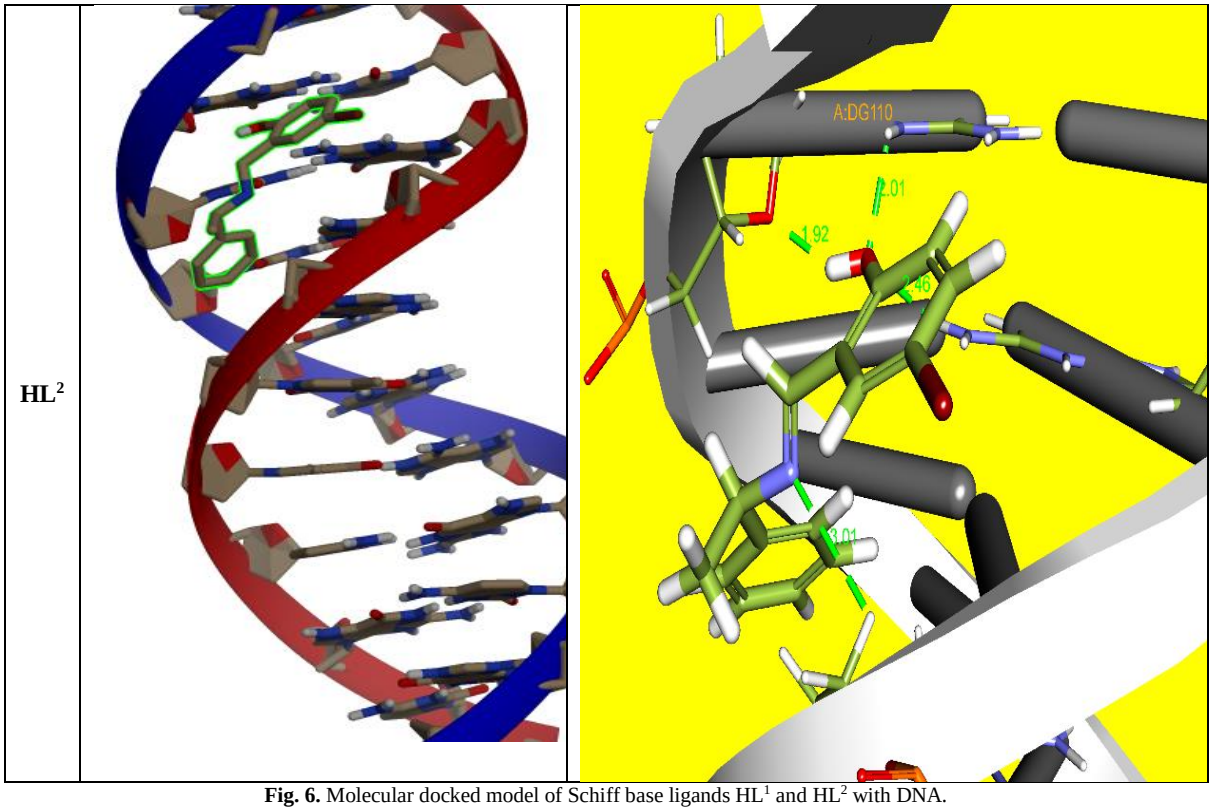

Fig. 6. Molecular docked model of Schiff base ligands HL^1 and HL^2 with DNA.

Table 12. DNA docking results of the Schiff base ligands HL^1 and HL^2 (Unit: kcal/mol).

Ligand	Estimated Free Energy of Binding*	Final Intermolecular Energy	vdW + Hbond + desolv Energy	Electrostati Energy	Final Total Internal Energy	Torsional Free Energy	Unbound System's Energy
HL^1	-6.86	-8.23	-8.18	+0.08	-0.05	+1.37	-0.05
HL^2	-7.17	-8.27	-7.99	-0.27	-0.41	+1.1	-0.41

*$\Delta G_{binding} = \Delta G_{vdW+hb+desolv} + \Delta G_{elec} + \Delta G_{total} + \Delta G_{tor}$ ΔG_{unb}.

4. Conclusions

The present paper reports the synthesis and characterization of two Schiff base ligands that one of them was synthesizes for the first time. The structures of these Schiff base ligands were characterized on the basis of their FT-IR, UV-Vis, and ^{1}H-NMR data. The crystal and molecular structures of $HL^{1,2}$ Schiff base ligands were further elucidated by X-ray technique. Also, DFT calculation was done on $HL^{1,2,}$ where the calculated data showed were in close agreement with crystallographic data. Also, UV-Vis spectra of the ligands were investigated by TD-DFT and observed signals were determined. The comparison of energy gaps between HOMO and LUMO demonstrated that HL^2 had less energy gap, suggesting that HL^2 is a bit more active than HL^1. As it mentioned before, the energy gap between HOMO and LUMO demonstrates the molecular chemical stability. When this gap is low, the molecule has a excellent activity, chemical hardness, and lower reactivity. Moreover, the DNA docking studies suggested that the ligands HL^1 and the HL^2 fit into the minor and major grooves of the DNA helix.

5. Acknowledgements

We thank Semnan University for supporting this study.

References

[1] Zh. Yang, L. Wang, Zh. Zhou, Q. Zhou, Ch. Tang, Tetrahedron: *Asymmetry*, **12** (2001) 1579.

[2] K.C. Emregul, E. Duzgun, *O. Atakol, Corrosion Science*, **48** (2006) 3243.

[3] A. Prakash, D. Adhikari, *Int. J. ChemTech Res.* **3** (2011) 1891.

[4] K. Bhat, K.J. Chang, M.D. Aggarwal, W.S. Wang, B.G. Penn, D.O. Frazier, *Materials Chemistry and Physics*, **44** (1996) 261.

[5] M.P. Akerman, V.A. Chiazzari, *J. Mol. Struct.* **1058** (2014) 22.

[6] R.M. Issa, M. K. Awad, F.M. Atlam, *Materials and Corrosion*, 61 (2010) 709-714.

[7] Z. Parsaee, *J. Mol. Struct.* **1146** (2017) 644.

[8] S. Grimme, *Journal of Computational Chemistry*, **25** (2004) 1463.

[9] Q.T. That, K. Nguyen, P. Hansen, *Magnetic Resonance in Chemistry*, **43** (2005) 302.

[10] S. Sinnecker, L.D. Slep, E. Bill, F. Neese, *Inorg. Chem.* **44** (2005) 2245.

[11] S.D. George, T. Petrenko, F. Neese, *Inorg. Chim. Acta*, **361** (2008) 965.

[12] K. Ray, S.D.George, E.I. Solomon, K. Wieghardt, F. Neese, *Chem. Eur. J.* **13**(2007) 2783.

[13] S. Basak, D. Chopra, K.K. Rajak, Journal of Organometallic Chemistry, **693** (2008) 2649.

[14] M. Seth, T. Ziegler, *J. Chem. Phys.* **120** (2004) 10942.

[15] P. AdAo, J. Pessoa, R.T. Henriques, M.L. Kuznetsov, F. Avecilla, M.R. Maurya, U. Kumar, I. Correia, *Inorg. Chem.* **48** (2009) 3542.

[16] Z. Parsaee, Kh. Mohammadi, *J. Mol. Struct*. **1137** (2017) 512.

[17] C.M. da Silva, D.L. da Silva, L.V. Modolo, R.B. Alves, M.A. de Resende, C.V.B. Martins, A. de Fatima, *Journal of Advanced Research*, **2** (2011) 1.

[18] L. Shi, H. Ge, Sh. Tan, H. Li, Y. Song, H. Zhu, R. Tan, *European Journal of Medicinal Chemistry*, **42** (2007) 558.

[19] B.S. Creaven, B. Duff, D.A. Egan, K. Kavanagh, G. Rosair, V.R. Thangella, M. Walsh, *Inorg. Chim. Acta*, **363** (2010) 4048.

[20] G. Ceyhan, M. Kose, M. Tumer, I. Demirtas, A. Yaglioglu, V. McKee, *Journal of Luminescence*, **143** (2013) 623.

[21] K. Das, A. Datta, P. Liu, J. Huang, Ch. Hsu, W. Chang, B. Machura, Ch. Sinha, *Polyhedron*, **71** (2014) 85.

[22] A.A. El-Sherif, T.M.A. Eldebss, *Spectrochim. Acta, Part A*, **79** (2011) 1803.

[23] Sh.M. Sondhi, N. Singh, A. Kumar, O. Lozachc, L. Meijer, *Bioorganic & Medicinal Chemistry*, **14** (2006) 3758.

[24] Z. Abbasi, M. Salehi, M. Kubicki, A. Khaleghian, *J. Coord. Chem.* **70** (2017) 2074.

[25] R. Fekri, M. Salehi, A. Asadi, M. Kubicki, *Polyhedron*, **128** (2017) 175.

[26] H.-L. ZHU, X. -Y. LIU, Synth. React. *Inorg. Met. Org. Chem.* **35** (2005) 193.

[27] Jaworska, M., Wełniak, M., Zięciak, J., Kozakiewicz, A., Wojtczakb, A." Arkivoc **9** (2011) 189.

[28] CrysAlisPro 1.171.38.34a (Rigaku OD, 2015).

[29] A. Altomare, G. Cascarano, C. Giacovazzo and A. Gualardi, *J. Appl. Crystallogr.* **26** (1993), 343.

[30] G. M. Sheldrick, Acta Crystallogr., 2014, C71, 3.

[31] M.J. Frisch, et al., Gaussian 03, Revision B.03, Gaussian, Inc., Pittsburgh PA, 2003.

[32] J. B. Foresman, A. Frisch, Exploring Chemistry with Electronic Structure Meth Ods, 2nd ed., Gaussian Inc., Pittsburgh, PA, 1996.

[33] E.D. Glendening, A.E. Reed, J. E. Carpenter, F. Weinhold, NBO Version 3.1 TCI, University of Wisconsin, *Madison,* **65** (1998).

[34] N.S. Biradar, V.H. Kulkami, *J. Inorg. Nucl. Chem.* **33** (1971) 3781.

[35] J. N.R. Ruddick, J. R. Sams, *J. Organomet. Chem.* **60** (1973) 233.

[36] C. Cappelli, C. Duce, M. Formica, V. Fusi, L. Ghezzi, L. Giorgi, M. Micheloni, P. Paoli, P. Rossi, M. Rosaria Tine, *Inorg. Chim. Acta.* **417** (2014) 230.

[37] M. Amini, M. Khaksar, A. Arab, R. Masoomi Jahandizi, M. Bagherzadeh, D.M. Boghaei, A. Ellern, L.K. Woo, *Transition. Met. Chem.* **41** (2016) 97.

[38] A. Arab, F. Gobal, N. Nahali, M. Nahali, *J. Clust. Sci.* **24** (2013) 273.

[39] A. Arab, M. Habibzadeh, *Comput. Theor. Chem.* **1068** (2015) 52.

[40] F. Arjmand, Sh. Parveen, M..Afzal, M. Shahid,, *J. Photochem. Photobiol.* **114** (3) (2012) 15.